Water Science & Technology

Water Science & Technology Vol 87 No 8, 1879 doi: 10.2166/wst.2023.098

Assessment of the induced effect of selected iron hydroxysulfates biosynthesized using *Acidithiobacillus ferrooxidans* for biomineralization of acid mine drainage

Heru Wang[a,†], Qian Guo[b,†], Zehao Guo[b], Haowei Luo[b], Honghu Li[b], Jun Yang[b,c] and Yongwei Song[b,*]

[a] Laboratory Centre for Safety and Environment, Zhongnan University of Economics and Law, Wuhan 430073, China
[b] Department of Environmental Engineering, School of Information and Safety Engineering, Zhongnan University of Economics and Law, Wuhan 430073, China
[c] Institute of Environmental Management and Policy, Zhongnan University of Economics and Law, Wuhan 430073, China
*Corresponding author. E-mail: songyongwei@zuel.edu.cn
†These authors contributed equally to this work (E-mail: z0004382@zuel.edu.cn; qian123821@163.com).

YS, 0000-0001-9935-1131

ABSTRACT

Soluble iron and sulfate in acid mine drainage (AMD) can be greatly removed through the formation of minerals facilitated by seed crystals. However, the difference in the effects of jarosite and schwertmannite as endogenous seed crystals to induce AMD mineralization remains unclear. This paper intends to study the effect of Fe^{2+} oxidation and Fe^{3+} mineralization in the biosynthesis of minerals using different addition amounts and methods of jarosite or schwertmannite. The results showed that the addition amount and method of different seed crystals had no effect on the Fe^{2+} bio-oxidation but would change the Fe^{3+} mineralization efficiency. With the same amount of seed crystals added, jarosite exhibited a higher capacity to promote Fe^{3+} mineralization than schwertmannite. Adding seed crystals before the initiation of Fe^{2+} oxidation (0 h) could significantly promote Fe^{3+} mineralization efficiency. With the increase of seed crystals, jarosite could not only shorten the time required for mineral synthesis but also improve the final mineral yield, whereas schwertmannite could only shorten the time required for mineral synthesis. When Fe^{2+} was completely oxidized to Fe^{3+} (48 h), the supplementary of jarosite could still effectively improve Fe^{3+} mineralization efficiency, but the addition of schwertmannite no longer affected the final mineralization degree.

Key words: *Acidithiobacillus ferrooxidans*, acid mine drainage, biomineralization, jarosite, schwertmannite, seed crystals

HIGHLIGHTS

- The addition of jarosite and schwertmannite had no significant effect on the bio-oxidation of Fe^{2+} by *A. ferrooxidans* but would change the mineralization efficiency of Fe^{3+}.
- The effect of jarosite addition on the mineralization of Fe^{3+} was much greater than that of schwertmannite addition.
- Adding seed crystals before the initiation of Fe^{2+} oxidation could significantly promote Fe^{3+} mineralization efficiency.

GRAPHICAL ABSTRACT

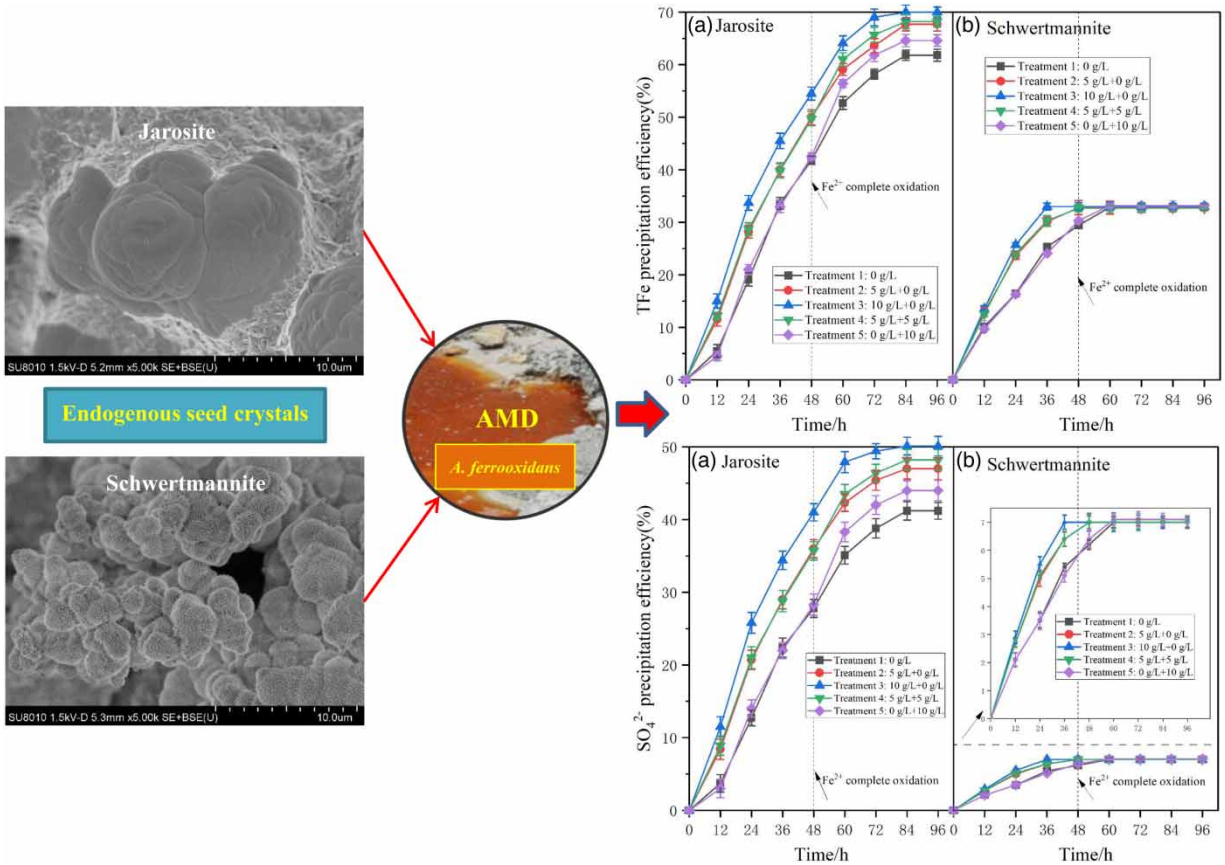

1. INTRODUCTION

Many sulfide mineral tailings are produced during the development and utilization of mineral resources (Huang *et al.* 2020; Hu *et al.* 2021). The accumulated tailings are exposed and react with oxygen and water in the air under the action of microorganisms, producing a large amount of acid mine drainage (AMD) rich in Fe^{2+}, Fe^{3+}, SO_4^{2-}, and other heavy metals (such as Cu, Cr, and Cd; Akcil & Koldas 2006; Song *et al.* 2022). Moreover, a significant amount of H^+ is produced in the formation of AMD, and the pH of the drainage is generally approximately 2–4 (Tabelin *et al.* 2018, 2020). Acid and heavy metals are the main pollutants in AMD, which cause great harm to the environment and human health (Kefeni *et al.* 2017). Neutralization is currently the most common method of treating AMD (Wang *et al.* 2019), and engineering utilization accounts for more than 90% of its application (Herrera *et al.* 2007). By adding an alkaline neutralizer to AMD, heavy metals could react with OH^- to form hydroxide precipitation under alkaline conditions, which could be removed by filtering.

Additionally, the pH of the drainage is increased at the same time to achieve the purpose of AMD treatment. Currently, lime or limestones are the most commonly used neutralizers. Neutralization can treat AMD of any concentration and nature, and it has the advantages of mature technology, simple operation, excellent adaptability, and good treatment effect (Markovic *et al.* 2020). However, a large amount of toxic waste residue, consisting of $CaSO_4$, $Fe(OH)_3$, and toxic metal oxides, is produced in this method, which will easily cause secondary pollution to the environment if not treated properly. Therefore, finding a new environmentally friendly AMD treatment method is of great significance.

Acidithiobacillus ferrooxidans (*A. ferrooxidans*) is a chemoautotrophic bacterium that widely exists in AMD. It mainly obtains energy by oxidizing Fe^{2+}, thereby fixing the carbon source in the air to promote its own growth without other energy sources (Raquel *et al.* 2007). In recent years, many studies have shown that the content of heavy metals in AMD is significantly lower than the theoretical value during the discharge process, and it is also accompanied by the natural passivation of arsenic (Gagliano *et al.* 2003; Regenspurg & Peiffer 2005). That is because Fe^{3+} biooxidized by Fe^{2+} under the action

of *A. ferrooxidans* is further hydrolyzed to form secondary iron hydroxysulfate minerals (Egal *et al.* 2009). As a result, Fe^{2+}, Fe^{3+}, H^+, and SO_4^{2-} were consumed in the process, and the content of heavy metals in AMD was greatly reduced by the adsorption and coprecipitation of secondary iron minerals. In neutralization, as Fe^{2+} needs to be precipitated at a high pH, it usually needs to be converted to Fe^{3+} by preparation before adding lime. Using the bio-oxidation of *A. ferrooxidans*, Fe^{2+} can be rapidly and completely oxidized, which reduces the processing time. Moreover, most metal and sulfate ions in the solution were removed via hydrolysis precipitation, which greatly reduced the amount of lime added in the subsequent neutralization treatment; therefore, only a small amount of calcium sulfate needs secondary treatment. Furthermore, the secondary iron minerals produced in the process can be used as environmental adsorption materials after collection (Xiong *et al.* 2008; Song *et al.* 2014). Due to the advantages of prebiomineralization by *A. ferrooxidans*, many scholars have investigated how to consciously regulate and strengthen the biomineralization process and apply it to water treatment in recent years (Zhou 2017; Naidu *et al.* 2019; Wang *et al.* 2019, 2021; Song *et al.* 2022). For instance, Zhou (2017) develops a novel passive biomineralization–limestone ditch treatment system through several oxidation–reduction cycles via *A. ferrooxidans* and Acidiphilic iron-reducing bacteria. Song *et al.* (2022) purposed an approach for treating AMD using a cyclic bio-oxidation and electroreduction process.

Secondary iron minerals in AMD are mainly schwertmannite and jarosite, both of which are formed under acidic conditions (Equations (1)–(3); Bai *et al.* 2012).

$$4Fe^{2+} + 4O_2 + 4H^+ \rightarrow 4Fe^{3+} + 2H_2O + \text{enerage } (A.\ ferrooxidans \text{ action}) \quad (1)$$

$$8Fe^{3+} + SO_4^{2-} + 14H_2O \rightarrow Fe_8O_8(OH)_6SO_4 \text{ (schwertmannite)} + 22H^+ \quad (2)$$

$$K^+ + 3Fe^{3+} + 2SO_4^{2-} + 6H_2O \rightarrow KFe_3(SO_4)_2(OH)_6 \text{ (jarosite)} + 6H^+ \quad (3)$$

Schwertmannite and jarosite have excellent adsorption and coprecipitation effects on heavy metals and metalloids, and developing them as a new type of environmental mineralogy materials for AMD treatment is of great environmental significance and application value. Promoting the mineralization ability of various ions is a new direction for the treatment of AMD (Bao *et al.* 2018). However, there remain many defects in the biosynthesis of secondary iron minerals. For example, the yield of schwertmannite synthesis is low; hence, the removal effect of ions and SO_4^{2-} in solution is not ideal. This research focuses on obtaining a large amount of secondary iron minerals in a short time to effectively remove metal ions and SO_4^{2-} in the solution. In recent years, some scholars have proposed adding crystal seeds in a simulated AMD environment to stimulate mineralization through seed induction and have conducted a series of experiments. For example, Wang & Zhou (2011) reported the removal of soluble ferrous iron in AMD through the formation of biogenic iron oxysulfate precipitates facilitated by diatomite and quartz sand. However, the promoting effect of those two kinds of exogenous seeds is relatively slow, and the obtained products are often mixed with impurities, which are difficult to separate. Therefore, schwertmannite and jarosite were selected as exogenous seeds to study the effect of their addition on the formation of sulfate iron minerals in AMD environments. Wang *et al.* used jarosite as a seed crystal for the first time and studied the effect of its addition on jarosite formation in an AMD environment (Wang *et al.* 2013). The results show that jarosite can effectively promote the formation of sulfate iron minerals through seed crystal stimulation. However, there is currently no report on the effect of schwertmannite as a seed crystal on mineral formation. The difference in the effect of the two minerals as seed crystals to induce mineralization is unclear, and their mechanism of action is unknown.

Therefore, this study intends to add endogenous crystal seeds, schwertmannite and jarosite, to a simulated AMD environment under optimized conditions according to the previous research results and to examine the effects of their addition amount and addition method on Fe^{2+} oxidation and Fe^{3+} mineralization in the biosynthesis of secondary iron hydroxysulfate minerals. Moreover, this study aims to analyze the influence mechanism and provide optimized conditions and theoretical guidance for iron and SO_4^{2-} removal in AMD.

2. MATERIALS AND METHODS

2.1. Preparation of *A. ferrooxidans* resting cell suspensions

A. ferrooxidans bacteria were obtained from China General Microbiological Culture Collection Center (CGMCC) and the accession no. was CGMCC No. 0727, which were cultured in a 9K medium developed by Silverman & Lundgren (1959)

and refrigerated at 4 °C. The components (analytically pure) of the medium were as follows: 1-L deionized water, 3.00 g of $(NH_4)_2SO_4$, 0.10 g of KCl, 0.50 g of K_2HPO_4, 0.50 g of $MgSO_4{\cdot}7H_2O$, and 0.01 g of $Ca(NO_3)_2$. Before the experiment, to prevent the *A. ferrooxidans* cells from being inactive due to prolonged refrigeration, they were resuscitated first, and the culture was expanded to the amount required for the experiment (Liao *et al.* 2009). Briefly, in a series of 250 mL Erlenmeyer flasks, 15 mL of the refrigerated bacterial suspensions was inoculated into a 9K liquid medium, keeping the total reaction volume at 150 mL. Furthermore, 6.63 g $FeSO_4{\cdot}7H_2O$ was added as an energy substance. After shaking it to dissolve, we adjusted the system's pH to 2.50 with 1:1 H_2SO_4. The Erlenmeyer flasks were then incubated in a shaker at 28 °C and 180 rpm until the late logarithmic growth phase was reached (approximately 72 h). Finally, the cultured suspensions were filtered through a Whatman No. 4 filter paper to remove the iron hydroxysulfate mineral precipitates formed during the cultivation process. The filtrates were centrifuged at 10,000 × g for 10 min to precipitate bacterial cells, which were then washed three times with acidic deionized water (pH 2.00) and pure water to remove various heavy metal ions. Next, these cells were suspended with H_2SO_4 (pH 2.50), and finally, *A. ferrooxidans* resting cell suspensions were obtained.

2.2. Biosynthesis and process analysis of jarosite and schwertmannite

Biosynthesis of jarosite was performed by oxidizing $FeSO_4$ with *A. ferrooxidans* cells in the presence of K^+, as reported by Bai *et al.* (2012). The most suitable conditions for the formation of jarosite by biomineralization were adopted for the synthesis, including the initial pH, temperature, inoculation amount of bacteria, initial Fe^{2+} concentration, and Fe/K molar ratio (Bai & Zhou 2011a, 2011b; Song *et al.* 2018). Briefly, in a series of 500 mL Erlenmeyer flasks, 30 mL of *A. ferrooxidans* cell suspensions was introduced to a solution containing 13.26 g $FeSO_4{\cdot}7H_2O$ and 1.38 g of K_2SO_4 with a Fe/K molar ratio of 3:1. Then, deionized water was added to keep the total reaction volume at 300 mL. The system's pH was adjusted to 2.50 with 1:1 H_2SO_4. The above flasks containing 10% (v/v) inoculum and $FeSO_4$ were subsequently incubated in a shaker at 28 °C and 180 rpm. After reaction for 96 h, the yellow minerals formed in the systems were harvested by filtering through a Whatman No. 4 filter paper. We washed them three times with acidic deionized water (pH 2.00) and pure water to remove soluble impurities. Finally, we dried them at 50 °C to constant weight and stored them in a desiccator for later use. A certain amount of minerals was identified using a scanning electron microscope (SEM) and X-ray diffraction (XRD).

By oxidizing $FeSO_4$ with *A. ferrooxidans* cells, biogenic schwertmannite can be synthesized according to the method described by Liao *et al.* (2009). Furthermore, the most suitable conditions for the formation of schwertmannite had been adopted (Song *et al.* 2018). Briefly, in a series of 500 mL Erlenmeyer flasks, 30 mL of *A. ferrooxidans* cell suspensions was introduced to a solution containing 13.26 g of $FeSO_4{\cdot}7H_2O$. Then, deionized water was added to keep the total reaction volume at 300 mL. Next, we adjusted the system's pH to 2.50 with 1:1 H_2SO_4. The above flasks containing 10% (v/v) inoculum and $FeSO_4$ were subsequently incubated in a shaker at 28 °C and 180 rpm. The red minerals formed in the solution were collected via filtration in the same manner and identified via SEM and XRD.

2.3. Jarosite and schwertmannite promote secondary iron mineral synthesis in simulated AMD

For the experiment of induced mineral synthesis by jarosite, briefly, in a series of 250 mL Erlenmeyer flasks, 15 mL of *A. ferrooxidans* cell suspensions were added to a solution containing 6.63 g of $FeSO_4{\cdot}7H_2O$ and 0.69 g of K_2SO_4 with a Fe/K molar ratio of 3:1. Then, deionized water was added to keep the total reaction volume at 150 mL. Next, the system's pH was adjusted to 2.50 with 1:1 H_2SO_4 to obtain a synthetic solution of jarosite. According to the addition amount and addition method of the presynthesized jarosite listed in Table 1, five different treatments were arranged as follows: Treatment 1 was the abovementioned jarosite synthesis solution; Treatment 2 was the jarosite synthesis solution with 5 g/L jarosite seed crystals added before the initiation of Fe^{2+} oxidation; Treatment 3 was the jarosite synthesis solution with 10 g/L jarosite seed crystals added before the initiation of Fe^{2+} oxidation; Treatment 4 was the jarosite synthesis solution with 5 g/L jarosite seed crystals added before the initiation of Fe^{2+} oxidation and after the oxidation was complete. Treatment 5 was the jarosite synthesis solution with 10 g/L jarosite seed crystals added after the Fe^{2+} oxidation was complete. Each treatment was performed in triplicate, and all Erlenmeyer flasks were subsequently incubated in a shaker at 28 °C and 180 rpm.

For the experiment of induced mineral synthesis by schwertmannite, briefly, in a series of 250 mL Erlenmeyer flasks, 15 mL of *A. ferrooxidans* cell suspensions was added to a solution containing 6.63 g of $FeSO_4{\cdot}7H_2O$. Then, deionized water was added to keep the total reaction volume at 150 mL. Next, the system's pH was adjusted to 2.50 with 1:1 H_2SO_4 to obtain a synthetic solution of schwertmannite. According to the addition amount and addition method of the presynthesized

Table 1 | Designed addition amount and addition method of the presynthesized jarosite or schwertmannite in each treatment solution

Treatment	Amount of jarosite or schwertmannite added before the initiation of Fe^{2+} oxidation (g/L)	Amount of jarosite or schwertmannite added after complete oxidation of Fe^{2+} (g/L)
1	0	0
2	5	0
3	10	0
4	5	5
5	0	10

schwertmannite, five different treatments were arranged as listed in Table 1. Each treatment was performed in triplicate, and all Erlenmeyer flasks were subsequently incubated in a shaker at 28 °C and 180 rpm.

The pH, Fe^{2+} concentration, TFe concentration, and SO_4^{2-} concentration of each Erlenmeyer flask were dynamically monitored by taking a 2 mL sample filtered through a 0.22 μm membrane and subsequently converting Fe^{2+} oxidation efficiency, TFe precipitation efficiency, and SO_4^{2-} precipitation efficiency. After reaction for 96 h, the jarosite or schwertmannite produced in each treatment was harvested by filtering through a Whatman No. 4 filter paper. We washed them three times with acidic deionized water (pH 2.00) and pure water to remove soluble impurities and finally dried them at 50 °C. Then, we calculated and compared the net dry weight of jarosite or schwertmannite in each treatment solution.

2.4. Analytical methods

The pH of the solution was measured using a digital pH meter (pHS-3C, China). The Fe^{2+} and TFe concentrations were determined using the 1,10-phenanthroline method (APHA 2005). When it was necessary to distinguish between Fe^{3+} and Fe^{2+}, Fe^{2+} concentration was measured before and after reduction using excess ascorbic acid, and Fe^{3+} concentration was calculated based on the difference between the two measurements. Other metal elements were determined using a Shimadzu ICPS-7500 inductively coupled plasma atomic emission spectrometer (ICP-AES; Shimadzu, Japan; Todolí & Mermet 2006). The SO_4^{2-} concentration was determined using barium chromate spectrophotometry (ASTM 2005). A SU8010 SEM (Hitachi, Japan) was used to observe the mineral morphologies (Weaver *et al.* 2010). The crystal structures of the collected minerals were determined using an X-ray diffractometer (Bruker D8, Germany; Fewster 2004).

Fe^{2+} oxidation efficiency, TFe precipitation efficiency, and SO_4^{2-} precipitation efficiency were converted according to the Fe^{2+}, TFe, and SO_4^{2-} concentrations. The calculation formula is as follows:

$$Fe^{2+}\text{oxidation efficiency} = \frac{c(Fe^{2+})_0 - c(Fe^{2+})_t}{c(Fe^{2+})_0} \times 100\%,$$

$$\text{TFe precipitation efficiency} = \frac{c(TFe)_0 - c(TFe)_t}{c(TFe)_0} \times 100\%,$$

$$SO_4^{2-}\text{precipitation efficiency} = \frac{c(SO_4^{2-})_0 - c(SO_4^{2-})_t}{c(SO_4^{2-})_0} \times 100\%,$$

where $c(Fe^{2+})_0$, $c(TFe)_0$, and $c(SO_4^{2-})_0$ refer to Fe^{2+}, TFe, and SO_4^{2-} concentrations, respectively, in the solution at the beginning of the reaction, whereas $c(Fe^{2+})_t$, $c(TFe)_t$, and $c(SO_4^{2-})_t$ refer to Fe^{2+}, TFe, and SO_4^{2-} concentrations, respectively, in the solution after t hours of reaction.

3. RESULTS

3.1. Identification of biosynthesized jarosite and schwertmannite

Yellow minerals were formed in the solution containing $FeSO_4$ and K_2SO_4, whereas red minerals were formed during the oxidation of $FeSO_4$ by *A. ferrooxidans* in the solution containing $FeSO_4$ alone. It can be seen from SEM images (Figure 1) that the yellow minerals comprised agglomerated particles with smooth surfaces, and the red minerals comprised spherical particles with a 'hedgehog' morphology on the particle surface. Figure 2 depicts the XRD patterns of these two minerals. The

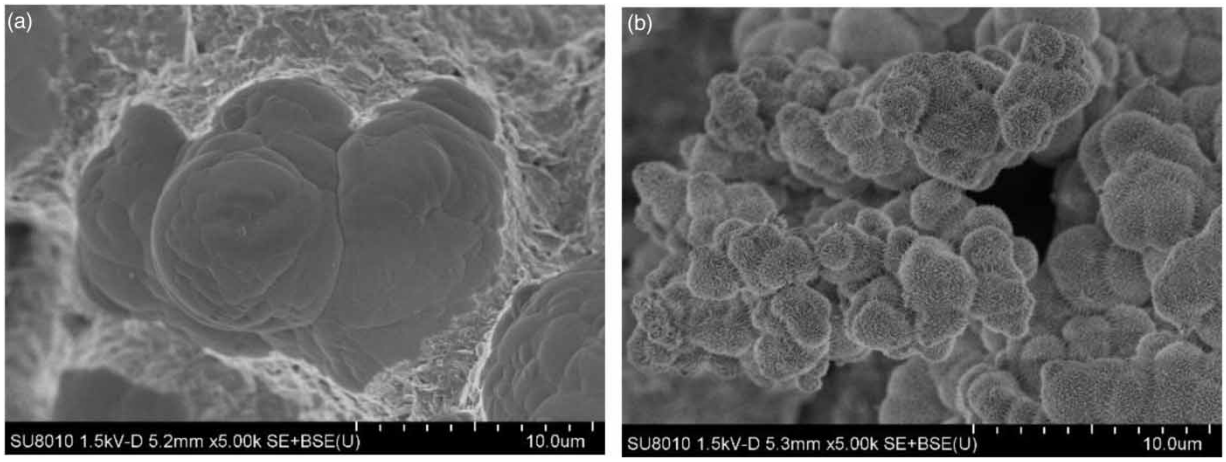

Figure 1 | SEM images of biosynthesized (a) jarosite and (b) schwertmannite.

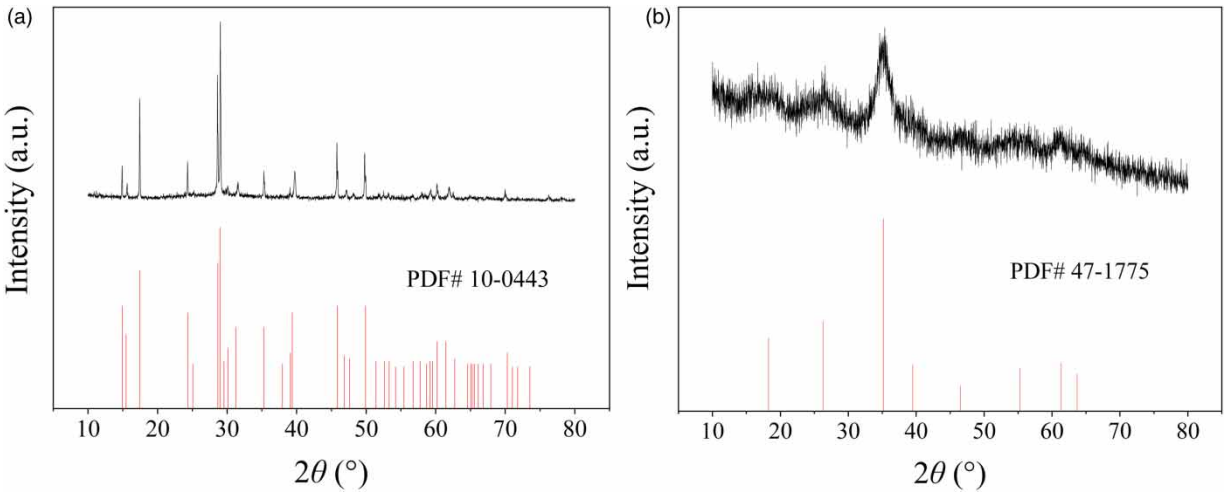

Figure 2 | XRD of biosynthesized (a) jarosite and (b) schwertmannite.

XRD results of yellow minerals demonstrated a good crystalline structure because of the strong and sharp diffraction peaks (the key diffraction peaks $2\theta = 14.93°, 17.41°, 24.37°, 28.97°, 35.28°, 39.37°, 45.86°, 49.93°$), and these peaks matched those of the standard diffraction data for jarosite (JCPDS No. 10-0443). However, the XRD pattern of red minerals exhibited a weak crystalline structure with eight broad characteristic peaks ($2\theta = 18.24°, 26.27°, 35.16°, 39.49°, 46.53°, 55.29°, 61.34°, 63.69°$) and all diffraction peaks highly matched those of the standard diffraction data for schwertmannite (JCPDS No. 47-1775), suggesting that the red minerals are pure schwertmannite. These results are consistent with previous studies that the oxidation of $FeSO_4$ by *A. ferrooxidans* results in the formation of jarosite when a high concentration of K^+ or NH_4^+ is present (Bai *et al.* 2012; Jones *et al.* 2014), whereas schwertmannite can be formed during the oxidation of $FeSO_4$ by *A. ferrooxidans* in a solution containing $FeSO_4$ alone (Song *et al.* 2022). The chemical formula of the jarosite or schwertmannite could be expressed as $KFe_{3.21}(SO_4)_{1.58}(OH)_{6.14}$ or $Fe_8O_8(OH)_{4.36}(SO_4)_{1.84}$, respectively, according to the molar ratio of SO_4/Fe and K/Fe determined by Inductively Coupled Plasma-Atomic Emission Spectrometry and ion chromatography.

3.2. Dynamic changes of the pH, Fe^{2+}, TFe, and SO_4^{2-} concentrations in each induced system

3.2.1. Dynamic changes of Fe^{2+} oxidation efficiency in mineral synthesis systems with the addition of jarosite or schwertmannite

Figure 3 shows the dynamic changes of Fe^{2+} oxidation efficiency in each induced system added with jarosite or schwertmannite within 96 h. In the systems added with jarosite, the Fe^{2+} oxidation rate was not affected by the amount or method of seed

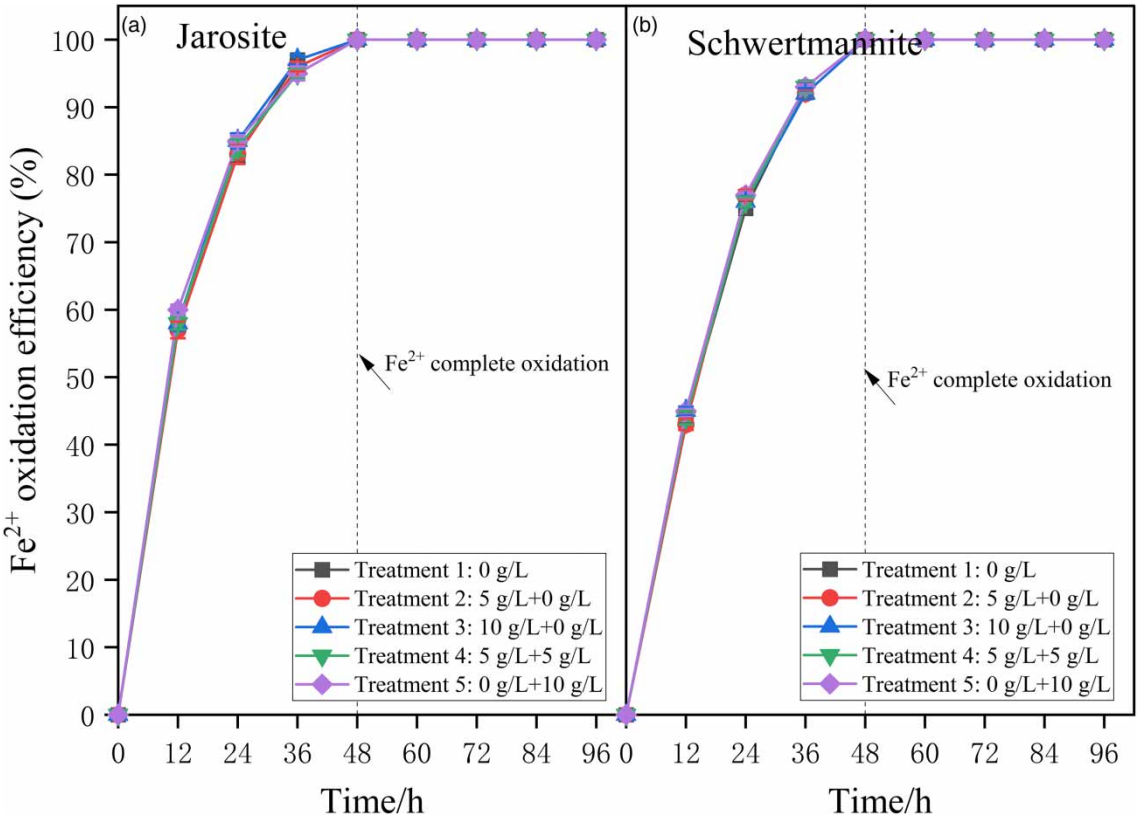

Figure 3 | Dynamic changes of Fe^{2+} oxidation efficiency in each mineral synthesis system with the addition of jarosite or schwertmannite.

crystal addition, and the five jarosite-treated solutions exhibited the same oxidation efficiency at the same time. The same is true for schwertmannite. Additionally, due to the action of *A. ferrooxidans*, Fe^{2+} in each system was completely oxidized within 48 h, whether it was added with jarosite or schwertmannite. Therefore, it can be considered that the addition of both jarosite and schwertmannite had no obvious effect on Fe^{2+} oxidation.

3.2.2. Dynamic changes of pH in mineral synthesis systems with the addition of jarosite or schwertmannite

Figure 4 shows the dynamic changes of pH in each induced system added with jarosite or schwertmannite within 96 h. For K_2SO_4–$FeSO_4$–H_2O systems added with jarosite, during the Fe^{2+} oxidation period (0–48 h), the more jarosite was added, the more the pH of the solution decreased. This was most obvious in 0–12 h. After 48 h of reaction, the pH of the synthetic solutions 'Treatment 1' and 'Treatment 5' without adding jarosite dropped to 2.04, whereas the pH of the synthetic solutions 'Treatment 2' and 'Treatment 4' added with 5 g/L jarosite dropped to 1.95. The pH of the synthetic solution 'Treatment 3' added with 10 g/L jarosite, which was the largest amount of jarosite added in the early stage of the reaction, dropped to 1.90. The addition of jarosite effectively promoted the hydrolysis and mineralization of Fe^{3+} at the initial stage of the reaction, and the pH of the solution was lower than that of the treatment solution without jarosite seeds.

After Fe^{2+} oxidation was complete (after 48 h), 5 and 10 g/L jarosite were added to 'Treatment 4' and 'Treatment 5,' respectively. At this time, although the addition of seed crystals could still stimulate mineralization and make the solution pH drop faster, the promoting effect was lower than that of adding before the initiation of Fe^{2+} oxidation. After 96 h of reaction, the pH of 'Treatment 1' without jarosite dropped to 1.82, and the pH of 'Treatment 2' added with 5 g/L jarosite only before the initiation of Fe^{2+} oxidation dropped to 1.75. 'Treatment 3,' 'Treatment 4,' and 'Treatment 5' were all added with a total amount of 10 g/L jarosite, but the pH of each treatment solution differed due to the influence of the addition method. The pH of 'Treatment 3' added with 10 g/L jarosite before the initiation of Fe^{2+} oxidation dropped to 1.73. The pH of 'Treatment 4,' in which 5 g/L jarosite was added twice before the initiation of Fe^{2+} oxidation and after the oxidation of Fe^{2+}, was complete and dropped to 1.75. The pH of 'Treatment 5' added with 10 g/L jarosite only after Fe^{2+} oxidation was complete, dropped to 1.79.

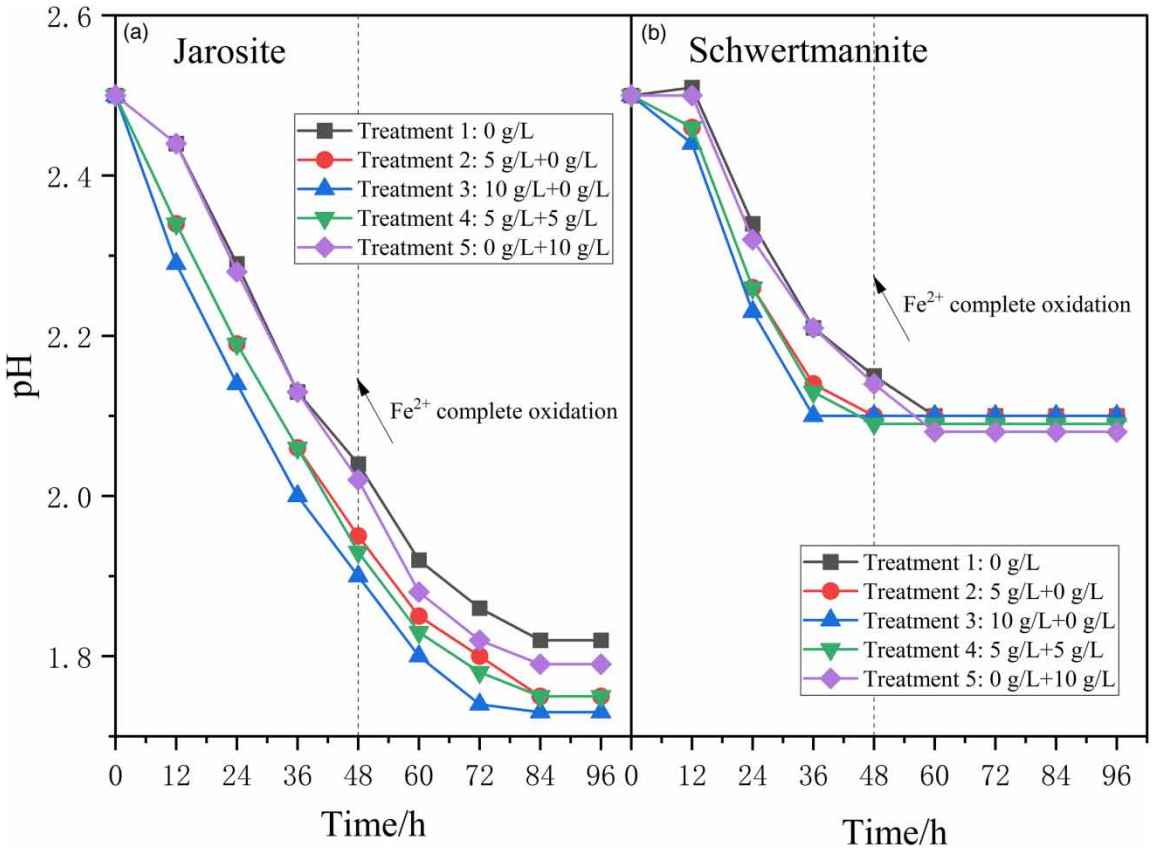

Figure 4 | Dynamic changes of pH in mineral synthesis systems with the addition of jarosite or schwertmannite.

For $FeSO_4$–H_2O systems added with schwertmannite, after 12 h, the pH of 'Treatment 1' and 'Treatment 5' without adding schwertmannite remained around 2.50. Conversely, the pH of the experimental group added with schwertmannite showed a significant downward trend. The more schwertmannite was added, the faster the pH dropped. Thereafter, with the prolongation of the reaction time, the hydrolysis of Fe^{3+} in the solution dominated, and the pH of each treatment solution decreased significantly. Studies have shown that the pH of the reaction system affects the synthesis of schwertmannite. When $pH < 2.10$, schwertmannite will no longer be synthesized in the solution, the hydrolysis of Fe^{3+} will be stagnant, and the pH of the solution will remain unchanged (Bigham *et al.* 1990). Therefore, the pH of all treatment solutions dropped to approximately 2.10 after a period of time and no longer changed; only the reaction time was different. The pH of 'Treatment 3' dropped to 2.10 at 36 h. Moreover, the pH of 'Treatment 2' and 'Treatment 4' reached 2.10 at 48 h. Conversely, the pH of 'Treatment 1' and 'Treatment 5' dropped to 2.10 at 60 h, which was the longest time.

3.2.3. Dynamic changes of TFe and SO_4^{2-} precipitation efficiencies in mineral synthesis systems with the addition of jarosite or schwertmannite

Figures 5 and 6 illustrate the changes in TFe and SO_4^{2-} precipitation efficiencies in each induced system added with jarosite or schwertmannite within 96 h, respectively.

For K_2SO_4–$FeSO_4$–H_2O systems added with jarosite, during the Fe^{2+} oxidation period (0–48 h), the only variable between the different solutions was the additional amount of jarosite. In this stage, the precipitation efficiency of TFe was significantly positively correlated with the amount of jarosite added, which was the most obvious in 0–24 h. After 48 h, the precipitation efficiency of TFe in 'Treatment 1' and 'Treatment 5' without adding jarosite was 41.8%, whereas that in 'Treatment 2' and 'Treatment 4' with 5 g/L jarosite added was approximately 50.0%. Furthermore, 'Treatment 3' added with 10 g/L jarosite, which was the largest amount of jarosite added in the early stage of the reaction, had the highest precipitation efficiency of 54.5% in 48 h. This had the same conclusion as the changing trend of pH in each treatment solution. That is, the addition

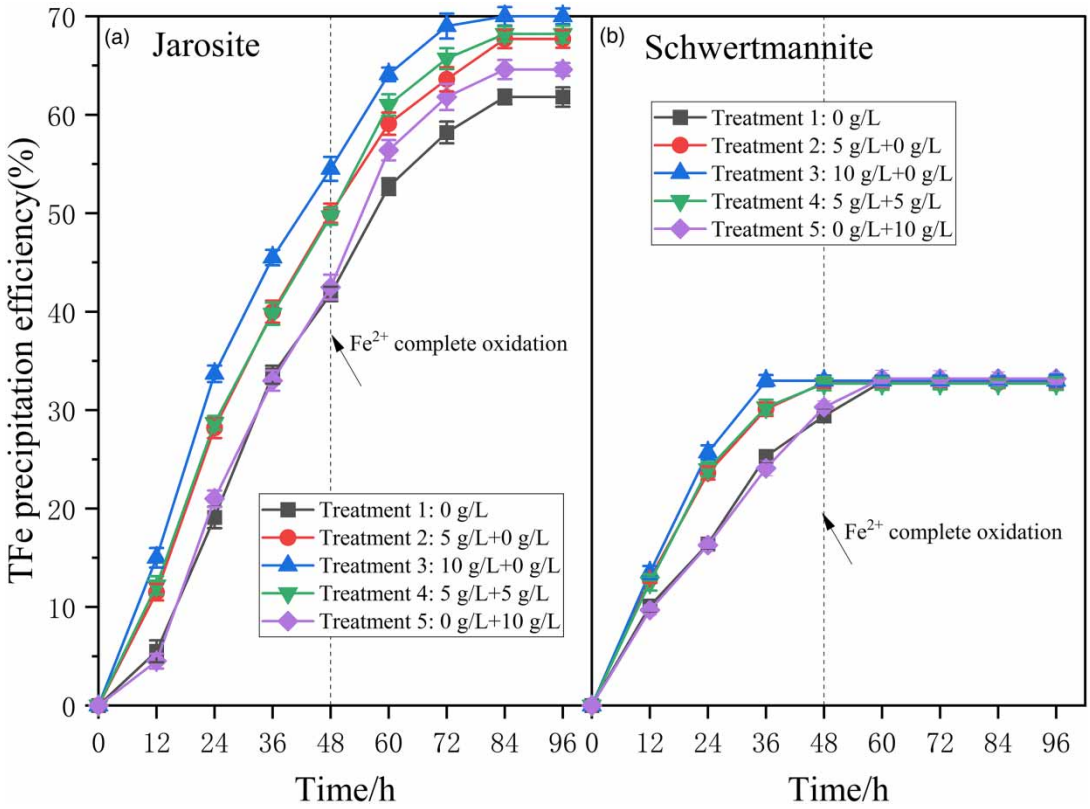

Figure 5 | Dynamic changes of TFe precipitation efficiency in mineral synthesis systems with the addition of jarosite or schwertmannite.

of jarosite effectively promoted the hydrolysis and mineralization of Fe^{3+} at the initial stage of the reaction, so that the pH of the solution was lower than that of the treatment solution without seed crystals added.

After 48 h, Fe^{2+} in the solution was completely oxidized, 5 and 10 g/L jarosite were added to 'Treatment 4' and 'Treatment 5,' respectively. Observing the trend of TFe precipitation efficiency after 48 h in the figure, we discovered that the addition of jarosite at this time could still promote the hydrolysis and mineralization of Fe^{3+}, increasing the precipitation efficiency of TFe. However, this promoting effect was not as significant as adding before the initiation of Fe^{2+} oxidation. After 96 h of reaction, the precipitation efficiency of 'Treatment 1' without jarosite added was 61.8%, and the precipitation efficiency of 'Treatment 2' with 5 g/L jarosite added only before the initiation of Fe^{2+} oxidation was 67.7%. 'Treatment 3,' 'Treatment 4,' and 'Treatment 5' were all added at a total amount of 10 g/L seed crystals, but the TFe precipitation efficiencies were not the same due to the influence of the addition method. The precipitation efficiency of 'Treatment 3' with 10 g/L jarosite added before the initiation of Fe^{2+} oxidation was 70.0%. Furthermore, the precipitation efficiency of 'Treatment 4,' in which 5 g/L jarosite was added twice before the initiation of Fe^{2+} oxidation and after Fe^{2+} oxidation, was 68.2%. The precipitation efficiency of 'Treatment 5' with 10 g/L jarosite added only after the oxidation of Fe^{2+} was 64.6%.

The synthesis of jarosite required the consumption of Fe^{3+} and SO_4^{2-}. The higher the TFe precipitation efficiency, the more jarosite synthesized and the more SO_4^{2-} consumed. Therefore, SO_4^{2-} and TFe precipitation efficiencies of each treatment solution had a similar changing trend, which together reflected the influence of jarosite addition on the hydrolysis and mineralization of Fe^{3+} in the system. After 96 h, the SO_4^{2-} precipitation efficiencies from 'Treatment 1' to 'Treatment 5' were 41.2, 47.0, 50.1, 48.2, and 44.0%, respectively.

For $FeSO_4$–H_2O systems added with schwertmannite, each treatment solution could reach the end of the reaction within 96 h and had the same TFe and SO_4^{2-} precipitation efficiencies, only the time required was different. 'Treatment 3' reached the end of the reaction at 36 h, 'Treatment 2' and 'Treatment 4' reached the end of the reaction at 48 h, whereas 'Treatment 1' and 'Treatment 5' ended the reaction at 60 h. Finally, the precipitation efficiency of TFe in each treatment solution was approximately 33.0%, and the precipitation efficiency of SO_4^{2-} was approximately 7.0%. The addition of schwertmannite in the

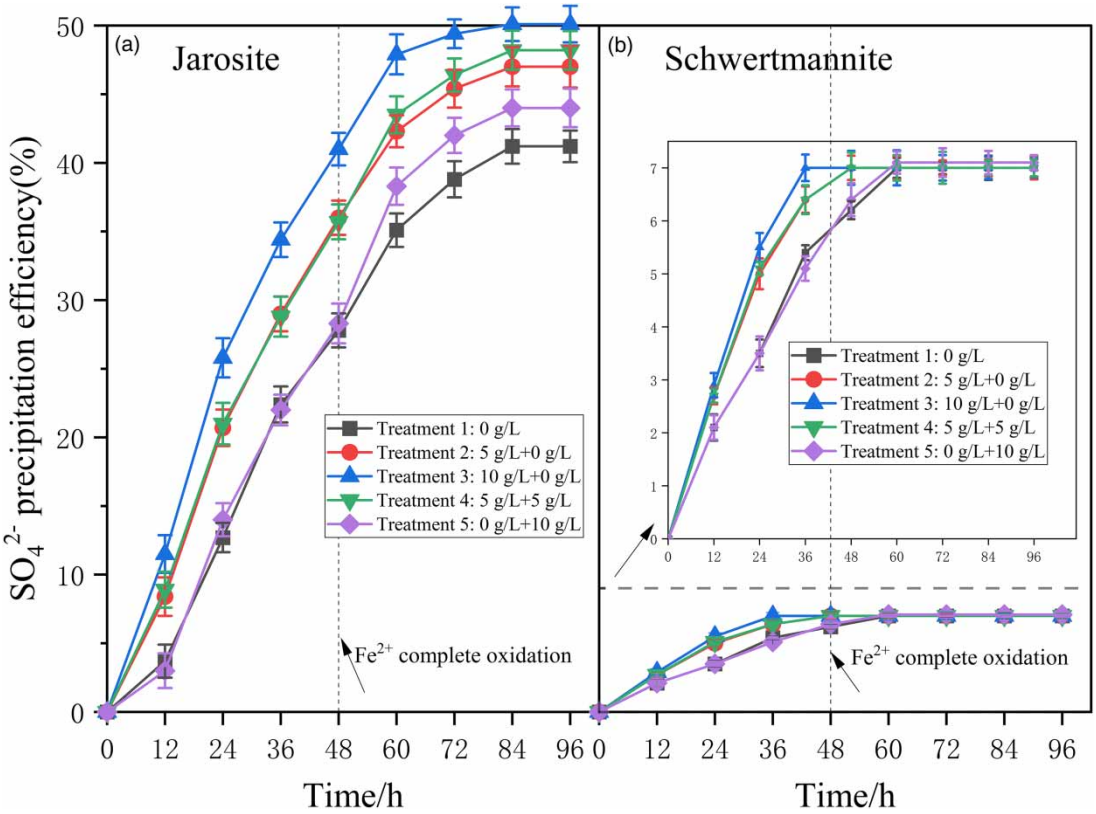

Figure 6 | Dynamic changes of SO_4^{2-} precipitation efficiency in mineral synthesis systems with the addition of jarosite or schwertmannite.

solution before the start of the reaction did not improve the degree of Fe^{3+} hydrolysis but effectively shortened the mineral synthesis time.

3.2.4. Dry weight of precipitates in mineral synthesis systems with the addition of jarosite or schwertmannite

After 96 h, jarosite or schwertmannite formed in each treatment solution was collected separately. After drying, the net mass of the resulting jarosite or schwertmannite in each treatment solution was calculated separately by weighing and subtracting the mass of the seed crystals added. Figure 7 shows the result obtained.

Figure 5 shows that the addition of jarosite before the initiation of Fe^{2+} oxidation effectively improved the mineral yield within 96 h, and it was significantly positively correlated with the amount of seed crystals added. After 96 h, compared with 'Treatment 1' without adding jarosite, the yields of 'Treatment 2' and 'Treatment 3' with 5 or 10 g/L jarosite added only before Fe^{2+} oxidation increased by 17.6 and 26.0%, respectively. The addition of jarosite after Fe^{2+} oxidation was complete had a certain promoting effect on mineral production, but this effect was lower than that of adding jarosite before the oxidation started. The yield of 'Treatment 4,' in which 5 g/L jarosite was added twice before the initiation of Fe^{2+} oxidation and after Fe^{2+} oxidation, increased by 16.2%, which was lower than that of the 'Treatment 3' solution. Furthermore, the yield of 'Treatment 5' with 10 g/L jarosite added only after Fe^{2+} oxidation increased by 4.0%, which was significantly lower than that of the 'Treatment 3' solution.

Since each treatment solution added with schwertmannite had the same TFe and SO_4^{2-} precipitation efficiencies at the end of the reaction, the dry weight of the resulting schwertmannite was basically the same. As shown in Figure 7, the dry weight of the schwertmannite produced in each treatment solution was approximately 0.75 g.

4. DISCUSSION

As the above results showed, the addition amount and method of jarosite or schwertmannite did not affect the Fe^{2+} oxidation efficiency by *A. ferrooxidans* but would change the hydrolysis and mineralization efficiency of the oxidation product Fe^{3+}.

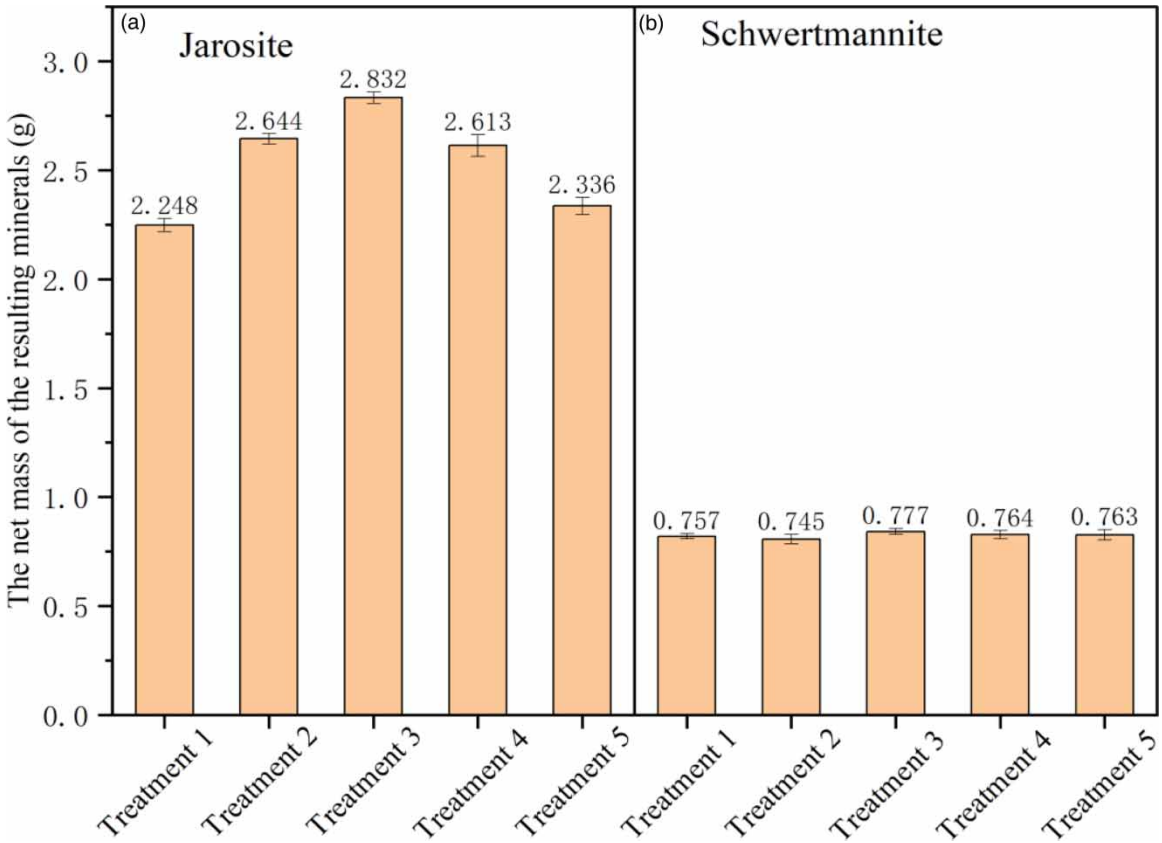

Figure 7 | Dry weight of jarosite or schwertmannite in each treatment solution.

However, there were some differences in the seed induction effect of the two minerals. With the same amount of seed crystals added, jarosite exhibited a much higher capacity to promote Fe^{3+} hydrolysis and mineralization than schwertmannite. Adding seed crystals before the initiation of Fe^{2+} oxidation (0 h) could significantly promote Fe^{3+} mineralization efficiency. With the increase of the additional amount of seed crystals, jarosite could not only shorten the time required for mineral synthesis but also improve the final mineral yield, whereas schwertmannite could only shorten the time required for mineral synthesis. When Fe^{2+} was completely oxidized to Fe^{3+} (48 h), the supplementary addition of jarosite could still effectively improve the hydrolysis and mineralization efficiency of Fe^{3+}, but the addition of schwertmannite no longer affected the final mineralization degree.

Gibbs free energy (G) is a crucial thermodynamic state function in physical chemistry, and the direction and limit in which various thermodynamic processes proceed spontaneously can be judged by the Gibbs free energy change (ΔG). The formation of biogenic secondary iron minerals mediated by *A. ferrooxidans* can be carried out at normal temperature and pressure (20–30 °C, ~101 kPa); it is scientific to use the standard molar Gibbs free energy ($\Delta_f G_m^0$) (25 °C, 100 kPa) as a criterion for the formation of biogenic secondary iron minerals. Therefore, this study is the first attempt to use G as the criterion to discuss the thermodynamic mechanism of the difference in the seed induction effect between jarosite and schwertmannite.

Table 2 shows the $\Delta_r G_m^0$ for different reactions (Robie & Hemingway 1995; Drouet & Navrotsky 2003; Majzlan *et al.* 2004). In a single Fe^{3+} system, $\Delta_r G_m^0 = 6.63\ \text{kJ·mol}^{-1} > 0$ (reaction (2)), the mineralization reaction cannot proceed spontaneously; that is, Fe^{3+} cannot directly combine with SO_4^{2-} to form schwertmannite. However, when K^+ with a strong ability to induce vitriol is present in the system, in the jarosite mineralization process, $\Delta_r G_m^0 = -22.20\ \text{kJ·mol}^{-1} < 0$ (reaction (3)); thus, the reaction could proceed spontaneously. However, due to the small $\Delta_r G_m^0$, the mineral synthesis process is relatively slow, and the effect of TFe and SO_4^{2-} precipitation is affected, which is consistent with the results in Figure 4. After coupling with Fe^{2+} oxidation by *A. ferrooxidans* (reaction (1)), the $\Delta_r G_m^0$ of ideal schwertmannite and ideal jarosite reached −34.12 and −67.45 kJ·mol^{-1}, respectively, satisfying the condition that the reaction proceeds spontaneously with $\Delta_r G_m^0 < 0$.

Table 2 | $\Delta_r G_m^0$ of different reactions

Reaction number	Equation	$\Delta_r G_m^0$ (kJ·mol^{-1})
(1)	$Fe^{2+}(aq) + 1/4O_2(g) + H^+(aq) = Fe^{3+}(aq) + 1/2H_2O(l)$	−45.25
(2)	$Fe^{3+}(aq) + 7/4H_2O(l) + 1/8SO_4^{2-}(aq) = 1/8Fe_8O_8(OH)_6SO_4(s) + 11/4H^+(aq)$	6.63
(3)	$1/3K^+(aq) + Fe^{3+}(aq) + 2/3SO_4^{2-}(aq) + 2H_2O(l) = 1/3KFe_3(SO_4)_2(OH)_6(s) + 2H^+(aq)$	−22.20
Schwertmannite	(1) + (2)	−34.12
Jarosite	(1) + (3)	−67.45

Therefore, the process of hydrolyzing Fe^{3+} to form schwertmannite can be spontaneously carried out, which cannot be achieved by itself. Additionally, the bio-oxidation of Fe^{2+} to synthesize jarosite is more favorable than schwertmannite.

In this study, we proposed the possibility of using jarosite and schwertmannite as crystal seeds to induce the rapid formation of minerals in a simulated AMD environment and obtained good results. However, this study was conducted as a laboratory simulation, not a pilot test. Furthermore, AMD has a complex composition and various metal ions; thus it is unclear whether it can produce similar results in wastewater. Moreover, this paper only discussed the first half of the treatment, i.e., biological mineralization, and did not study the following lime neutralization. The wastewater treatment was incomplete, and the advantages of lime neutralization over the traditional neutralization method were not realized. The reduced lime consumption cannot be calculated, including the analysis of economic benefits. Therefore, we can only say that it is possible to use minerals to induce mineralization, and their application to engineering needs further research.

5. CONCLUSIONS

The addition of jarosite and schwertmannite had no significant effect on the bio-oxidation of Fe^{2+} by *A. ferrooxidans*, but both could promote the hydrolysis of Fe^{3+} to form minerals. However, due to thermodynamic differences in the biosynthesis of jarosite and schwertmannite, the effect of seed stimulation was significantly different. The addition of jarosite can not only shorten the time required for mineral synthesis but can also effectively improve the mineral yield. However, the addition of schwertmannite can only shorten the mineral synthesis time. For the additional amount, the more the seed crystals added, the better the promoting effect. For the addition method, adding jarosite before and after Fe^{2+} oxidation could promote the hydrolysis and mineralization of Fe^{3+}. However, the addition of schwertmannite after Fe^{2+} oxidation was complete no longer had a promoting effect. This can be explained using the $\Delta_r G_m^0$ of jarosite and schwertmannite biosynthesis. At normal temperature and pressure, the reaction of Fe^{3+} hydrolysis to form jarosite has a negative $\Delta_r G_m^0$, whereas the reaction to form schwertmannite has a positive $\Delta_r G_m^0$. When coupled with the biological oxidation of Fe^{2+} by *A. ferrooxidans*, the resulting Fe^{3+} hydrolysis to form schwertmannite could occur spontaneously, exhibiting a negative $\Delta_r G_m^0$.

Furthermore, the formation of jarosite could show a larger negative $\Delta_r G_m^0$. Therefore, the effect of jarosite addition on the hydrolysis and mineralization of Fe^{3+} was much greater than that of schwertmannite addition, and the induction effect of schwertmannite was terminated together with the synthesis reaction after Fe^{2+} oxidation was complete. The finding of this study has important implications for the efficient removal of soluble iron and sulfate in AMD.

ACKNOWLEDGEMENTS

This work was supported by the National Natural Science Foundation of China (No. 21906183) and the Fundamental Research Funds for the Central Universities (No. 2722023BY020, 202351415).

AUTHORS' CONTRIBUTION

H.W. and Q.G. conceptualized methodology, designed this study, and wrote the original draft. Z.G., H.L., and H.L. carried out data curation and formal analysis. Y.S. and J.Y. wrote, reviewed and edited the original draft. All authors have read and agreed to the published version of the manuscript.

DATA AVAILABILITY STATEMENT

All relevant data are included in the paper or its Supplementary Information.

CONFLICT OF INTEREST

The authors declare there is no conflict.

REFERENCES

Akcil, A. & Koldas, S. 2006 Acid mine drainage (AMD): causes, treatment and case studies. *J. Cleaner Prod.* **14** (12–13), 1139–1145.

ASTM 2007 *Standard Test Method for Sulfate Ion in Water*. Designation: D516-2007, American Society of Testing Materials, West Conshohocken, PA

ASTM 2005 *Standard Test Method for Sulfate Ion in Water*. Designation: D516-16, American Society of Testing Materials.

Bai, S. & Zhou, L. 2011a Effects of microbial inoculation density and mineral collection time on the formation of secondary iron minerals in bioleach. *Chin. J. Microbiol.* **38** (04), 487–492.

Bai, S. & Zhou, L. 2011b Effects of monovalent cations and water-soluble organic matter on the formation of secondary iron minerals by bioleach. *Acta Mineral. Sin.* **31** (01), 118–125.

Bai, S., Xu, Z., Wang, M., Liao, Y., Liang, J., Zheng, C. & Zhou, L. 2012 Both initial concentrations of Fe(II) and monovalent cations jointly determine the formation of biogenic iron hydroxysulfate precipitates in acidic sulfate-rich environments. *Mat. Sci. Eng. C* **32** (8), 2323–2329.

Bao, Y., Guo, C., Lu, G., Yi, X., Wang, H. & Dang, Z. 2018 Role of microbial activity in Fe(III) hydroxysulfate mineral transformations in an acid mine drainage-impacted site from the Dabaoshan Mine. *Sci. Total Environ.* **616–617**, 647–657.

Bigham, J. M., Schwertmann, U., Carlson, L. & Murad, E. 1990 A poorly crystallized oxyhydroxysulfate of iron formed by bacterial oxidation of Fe(II) in acid mine waters. *Geochim. Cosmochim. Acta* **54** (10), 2743–2758.

Drouet, C. & Navrotsky, A. 2003 Synthesis, characterization, and thermochemistry of K-Na-H_3O jarosites. *Geochim. Cosmochim. Acta* **67** (11), 2063–2076.

Egal, M., Casiot, C., Morin, G., Parmentier, M., Bruneel, O., Lebrun, S. & Elbaz-Poulichet, F. 2009 Kinetic control on the formation of tooeleite, schwertmannite and jarosite by *Acidithiobacillus ferrooxidans* strains in an As(III)-rich acid mine water. *Chem. Geol.* **265** (3–4), 432–441.

Fewster, P. F. 2004 Advances in the structural characterisation of semiconductor crystals by X-ray scattering methods. *Prog. Cryst. Growth Charact. Mater.* **48/49**, 245–273.

Gagliano, W. B., Brill, M. R., Bigham, J. M., Jones, F. S. & Traina, S. J. 2003 Chemistry and mineralogy of ochreous sediments in a constructed mine drainage wetland. *Geochim. Cosmochim. Acta* **68** (9), 2119–2128.

Herrera, P., Uchiyama, H., Igarashi, T., Asakura, K., Ochi, Y., Iyatomi, N. & Nagae, S. 2007 Treatment of acid mine drainage through a ferrite formation process in central Hokkaido, Japan: evaluation of dissolved silica and aluminium interference in ferrite formation. *Miner. Eng.* **20** (13), 1255–1260.

Hu, B., Huang, L., Sun, X., Yang, S. & Tong, X. 2021 Research progress of mine wastewater treatment technology. *Conserv. Util. Min. Resour.* **41** (01), 46–52.

Huang, H., Wang, X., Chen, J. & Chen, C. 2020 Impact of pyrite tailings on the environment. *Chinese Soc. Environ. Sci.* **2020**, 5.

Jones, F. S., Bigham, J. M., Gramp, J. P. & Tuovinen, O. H. 2014 Synthesis and properties of ternary (K, NH_4, H_3O)-jarosites precipitated from *Acidithiobacillus ferrooxidans* cultures in simulated bioleaching solutions. *Mater. Sci. Eng. C* **44**, 391–399.

Kefeni, K. K., Msagati, T. A. M. & Mamba, B. B. 2017 Acid mine drainage: prevention, treatment options, and resource recovery: a review. *J. Cleaner Prod.* **151**, 475–493.

Liao, Y. H., Zhou, L. X., Liang, J. R. & Xiong, H. X. 2009 Biosynthesis of schwertmannite by *Acidithiobacillus ferrooxidans* cell suspensions under different pH condition. *Mater. Sci. Eng. C* **29** (1), 211–215.

Majzlan, J., Navrotsky, A. & Schwertamnn, U. 2004 Thermodynamics of iron oxides: part III. Enthalpies of formation and stability of ferrihydrite (~$Fe(OH)_3$), schwertmannite (~$FeO(OH)_{3/4}(SO_4)_{1/8}$), and ε-Fe_2O_3. *Geochim. Cosmochim. Acta* **68** (5), 1049–1059.

Markovic, R., Bessho, M., Masuda, N., Stevanovic, Z., Bozic, D., Trujic, T. A. & Gardic, V. 2020 New approach of metals removal from acid mine drainage. *Appl. Sci.* **10** (17), 5925.

Naidu, G., Ryu, S., Thiruvenkatachari, R., Choi, Y., Jeong, S. & Vigneswaran, S. 2019 A critical review on remediation, reuse, and resource recovery from acid mine drainage. *Environ. Pollut.* **247**, 1110–1124.

Raquel, Q., Claudia, L., Veloso, F. A., Pedroso, I., Holmes, D. S. & Jedlilcki, E. 2007 Bioinformatic prediction and experimental verification of fur-regulated genes in the extreme acidophile *Acidithiobacillus ferrooxidans*. *Nucleic Acids Res.* **35** (7), 2153–2166.

Regenspurg, S. & Peiffer, S. 2005 Arsenate and chromate incorporation in schwertmannite. *Appl. Geochem.* **20** (6), 1226–1239.

Robie, R. A. & Hemingway, B. S. 1995 *Thermodynamic Properties of Minerals and Related Substances at 298.15 K and 1 Bar (105 Pascals) Pressure and at Higher Temperatures*. Geological Survey Bulletin, Washington.

Silverman, M. P. & Lundgren, D. G. 1959 Studies on the chemoautotrophic iron bacterium *Ferrobacillus ferrooxidans*. I. An improved medium and a harvesting procedure for securing high cell yields. *J. Bacteriol.* **78**, 326–331.

Song, Y., Wang, M., Liang, J. & Zhou, L. 2014 High-rate precipitation of iron as jarosite by using a combination process of electrolytic reduction and biological oxidation. *Hydrometallurgy* **143**, 23–27.

Song, Y., Wang, H., Liang, J., Zhou, L., Cao, Y. & Zhou, J. 2018 Analysis of influencing factors on the formation of secondary iron minerals mediated by *A. ferrooxidans*. *Chin. J. Environ. Sci.* **38** (03), 1024–1030.

Song, Y., Guo, Z., Wang, R., Yang, L., Cao, Y. & Wang, H. 2022 A novel approach for treating acid mine drainage by forming schwertmannite driven by a combination of biooxidation and electroreduction before lime neutralization. *Water Res.* **221**, 118748.

Tabelin, C. B., Igarashi, T., Villacorte-Tabelin, M., Park, I., Opiso, E. M., Ito, M. & Hiroyoshi, N. 2018 Arsenic, selenium, boron, lead, cadmium, copper, and zinc in naturally contaminated rocks: a review of their sources, modes of enrichment, mechanisms of release, and mitigation strategies. *Sci. Total Environ.* **645**, 1522–1553.

Tabelin, C. B., Silwamba, M., Paglinawan, F. C., Mondejar, A. J. S., Duc, H. G., Resabal, V. J., Opiso, E. M., Igarashi, T., Tomiyama, S., Ito, M., Hiroyoshi, N. & Villacorte-Tabelin, M. 2020 Solid-phase partitioning and release-retention mechanisms of copper, lead, zinc and arsenic in soils impacted by artisanal and small-scale gold mining (ASGM) activities. *Chemosphere* **260**, 127574.

Todolí, J. L. & Mermet, J. M. 2006 Sample introduction systems for the analysis of liquid microsamples by ICP-AES and ICP-MS. *Spectrochim. Acta B: At. Spectrosc.* **61**, 239–283.

Wang, M. & Zhou, L. X. 2011 The removal of soluble ferrous iron in acid mine drainage (AMD) through the formation of biogenic iron oxyhydrosulfate precipitates facilitated by diatomite, quartz sand and potassium. *J. Rock Mineral.* **30** (06), 1031–1038.

Wang, M., Liang, J. R. & Zhou, L. X. 2013 The formation of biogenic jarosite by *Acidthiobacillus ferrooxidans* in the presence of crystal seed and potassium. *J. Nanjing Agric. Univ.* **36** (02), 97–102.

Wang, X., Jiang, H., Fang, D., Liang, J. & Zhou, L. 2019 A novel approach to rapidly purify acid mine drainage through chemically forming schwertmannite followed by lime neutralization. *Water Res.* **151**, 515–522.

Wang, X., Jiang, H., Zheng, G., Liang, J. & Zhou, L. 2021 Recovering iron and sulfate in the form of mineral from acid mine drainage by a bacteria-driven cyclic biomineralization system. *Chemosphere* **262**, 127567.

Weaver, J. C., Mershon, W., Zadrazil, M., Kooser, M. & Kisailus, D. 2010 Wide-field SEM of semiconducting minerals. *Mater. Today* **13**, 46–53.

Xiong, H., Liao, Y. & Zhou, L. 2008 Influence of chloride and sulfate on formation of akaganéite and schwertmannite through ferrous biooxidation by *Acidithiobacillus ferrooxidans* cells. *Environ. Sci. Technol.* **42** (23), 8681–8686.

Zhou, L. 2017 Biomineralization: a pivotal process in developing a novel passive treatment system for acid mine drainage. *Acta Chim. Sin.* **75** (06), 552–559.

First received 22 October 2022; accepted in revised form 23 March 2023. Available online 4 April 2023